

# Synthesis and investigation of BODIPYs with restricted *meso-*8-aryl rotation

Guanyu Zhang<sup>a</sup>, Maodie Wang<sup>a</sup>, Caroline Ndung'U<sup>a</sup>, Petia Bobadova-Parvanova\*<sup>b</sup>, Frank R. Fronczek<sup>a</sup>, Kevin M. Smith<sup>a</sup> and M. Graça H. Vicente\*<sup>a</sup>

<sup>a</sup>Department of Chemistry, Louisiana State University, Baton Rouge, LA 70803, USA <sup>b</sup>Department of Chemistry, Rockhurst University, Kansas City, MO 64110, USA

Dedicated to Professor Roberto Paolesse on the occasion of his 60th birthday.

Received 15 October 2019 Accepted 9 December 2019

**ABSTRACT**: Three BODIPYs bearing 1,3,5,7-tetramethyl substituents and a *meso*-8-aryl group were synthesized and investigated, both experimentally and computationally. The presence of the 1,7-methyl groups and of *ortho*-substituents on the *meso*-8-aryl ring prevent free rotation of the *meso*-8-aryl group, resulting in high fluorescence quantum yields. Substitution at the 2,6-positions of these BODIPYs with chlorine atoms causes pronounced red-shifted absorptions and emissions, and in the case of 2,6-dichloro-1,3,5,7-tetramethyl-8-(2,4,6-triphenylphenyl)-BODIPY **2c** increases its fluorescence quantum yields to 0.93 in dichloromethane and 0.98 in toluene. The X-ray structure of 1,3,5,7-tetramethyl-8-(2,4,6-triphenylphenyl)-BODIPY shows increased deviation from planarity and smaller dihedral angle of the *meso*-8-aryl group compared with the *meso*-8-phenyl- and *meso*-8-mesityl-BODIPY analogs. The presence of 2,6-chlorine atoms was found to not significantly affect the rotational barriers of the *meso*-8-aryl-groups.

**KEYWORDS**: BODIPY, aryl-rotation, fluorescence.

#### INTRODUCTION

4,4-Difluoro-4-bora-3a,4a-diaza-s-indacene (known as boron dipyrromethene or BODIPY) is an important class of fluorophore with multiple applications in fluorescence imaging due to its excellent spectroscopic properties, including large molar extinction coefficients, high fluorescence quantum yields, and high photostability [1–10]. The rapid increase in research interest of this type of dye has also arisen from its highly tunable physicochemical properties, which have resulted in the synthesis of BODIPY derivatives with a broad range of absorption and emission wavelengths. The modification of BODIPY has been explored by introducing various functional groups at the periphery of the dye, on both the carbon and boron atoms, using for example, electrophilic or nucleophilic substitution reactions

[11–15], metal-mediated cross-couplings [16–17], and Knoevenagel condensations [18–19]. In particular, functionalization at the meso-8-position has been achieved by Pd(0)-catalyzed cross-coupling reactions on 8-halogenated BODIPYs [17, 20–21]. The presence of an aryl group at the *meso*-8-position of the BODIPY usually has no significant effect on the absorption and emission wavelengths, due to the large dihedral angle it forms with the BODIPY core to minimize steric interactions with the 1,7-hydrogen atoms, but it can provide dyes with decreased fluorescence quantum yields, limiting their application in fluorescence imaging. This problem is largely attributed to the free rotation of the meso-aryl group, which reduces the loss of energy from the excited states via non-irradiative decay [20, 22]. To solve this problem, BODIPYs bearing meso-8-phenyl groups with ortho substituents (for example a mesityl group) and/or methyl groups at the 1,7-positions of the BODIPY have been synthesized to reduce the rotation of the meso-8-aryl group, showing restored emission, as shown in Fig. 1 [20, 22–23]. On the other hand, this drawback has also been

<sup>\*</sup>Correspondence to: Petia Bobadova-Parvanova, tel.: +816-501-4070, email: petia.bobadova@rockhurst.edu; M. Graça H. Vicente, tel.: +225-578-7405, email: vicente@lsu.edu.

# Fig. 1. BODIPYs with restricted *meso*-aryl rotation

Scheme 1. Synthesis of BODIPYs 1a-1c and 2a-2c

utilized in designing off-on BODIPY fluorescent probes for viscosity or temperature in biological research through rotation-restriction-induced emission enhancement mechanisms [24–26]. Herein, we report the synthesis and investigation of new sterically hindered BODIPYs bearing bulky *meso*-8-(2,4,6-triphenylphenyl) groups and 1,7-methyl substituents with restricted rotation of the *meso*-aryl group. The spectroscopic properties of these BODIPYs were investigated and compared with those of the *meso*-8-phenyl- and *meso*-8-mesityl-BODIPY derivatives, both experimentally and computationally.

### RESULTS AND DISCUSSION

# **Synthesis**

The synthetic routes to BODIPYs **1a–1c** and **2a–2c** are shown in Scheme 1. All BODIPYs were prepared, in 20–40% overall yields, by condensation of 2,4-dimethylpyrrole with the corresponding aryl aldehyde in the presence of trifluoroacetic acid (TFA),

followed by oxidation and boron complexation using boron trifluoride dietherate under basic conditions [27]. Treatment of BODIPYs **1a–1c** with 0.75 equivalent of trichlorocyanuric acid (TCCA) [17, 28–29] produced the corresponding 2,6-dichloro-BODIPYs **2a–2c** in 72–76% yields. The chlorination of BODIPYs **1a–1c** was clearly indicated by <sup>1</sup>H-NMR, due to the disappearance of the 2,6-hydrogen atoms at *ca*. 5.9 ppm. The structures of all BODIPYs were characterized by high resolution mass spectrometry and by <sup>1</sup>H- <sup>13</sup>C- and <sup>11</sup>B-NMR spectroscopy (see Figs S1–S9 in the Supporting information).

Restricted rotation and vibration

#### X-Ray analysis

A crystal of BODIPY 1c suitable for X-ray analysis was obtained by slow evaporation of dichloromethane and pentane, and the result is shown in Fig. 2. The 12-atom BODIPY core is slightly nonplanar, having a mean deviation of 0.058 Å and a slight twist about its longitudinal axis, such that the four methyl groups lie alternately above and below the plane by an average of

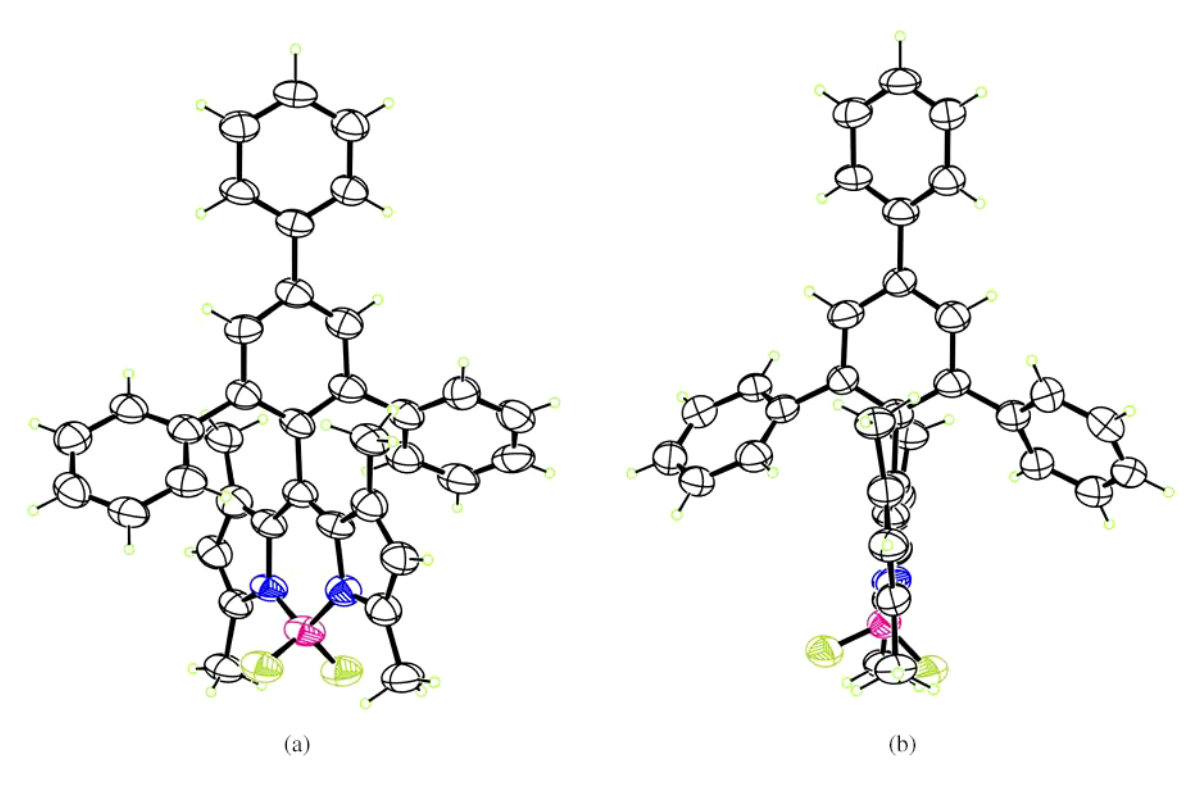


Fig. 2. X-ray crystal structure of BODIPY 1c; (a) top view and (b) side view with 50% ellipsoids

0.26 Å. The six atoms of the central  $C_3N_2B$  core of the BODIPY ring have a mean deviation from their best plane of 0.040 Å. The *meso*-phenyl ring forms a dihedral angle of 74.7° with the six-atom central BODIPY core. This dihedral angle is slightly smaller than the more nearly orthogonal ones seen in **1a** [16], 81.8° and **1b** [30], 85.5°. The performed computational studies confirm this effect; the dihedral angles in **1a** and **1b** are 90.0° and 90.1°, respectively, while that of **1c** is smaller at 79.8°. The central  $C_3N_2B$  rings of **1a** and **1b** are also more planar than those of **1c**, both with mean deviations of 0.021 Å.

#### **Spectroscopic properties**

The spectroscopic properties for BODIPYs 1a-1c and 2a-2c were investigated in dichloromethane, toluene and in a protic solvent (methanol), and the results obtained are summarized in Table 1 and shown in Fig. 3 (see also Figs S10 and S11). All BODIPYs exhibited a typical BODIPY absorption profile, characterized by a strong  $S0 \rightarrow S1$  transition peak centered at around 500 nm for 1a and 1b and 528 nm for 2a and 2b, along with a blue-shifted shoulder representing the vibrational transitions. BODIPYs 1c and 2c showed about 10 nm red-shifted absorptions relative to 1a and 1b and 2a and 2b, respectively, due to their smaller HOMO-LUMO energy gap (see Fig. 4). The 2,6-dichlorinated BODIPYs 2a-2c displayed significant red-shifted absorptions and emissions, by 21-27 nm, with a slightly increased Stokes shift by 3–5 nm relative to BODIPYs 1a–1c, as

previously observed for other 2,6-dichloro substituted BODIPYs [17, 29, 31]. This is attributed to the electron-withdrawing effect of the electronegative chlorine atoms, which removes electron density from the BODIPY core. Using the more polar solvent methanol instead of dichloromethane results in small (3–4 nm) blue (hypsochromic) shifts in both the maximum absorption wavelength and maximum emission wavelength, consistent with previous studies [32–33].

As expected, BODIPYs 1b and 1c bearing sterically hindered meso-aryl groups showed higher fluorescence quantum yields compared with BODIPY 1a due to increased restricted rotation of their meso-aryl groups compared with phenyl [22-23, 30]. On the other hand, BODIPY 1c displayed lower fluorescence quantum yields than BODIPY 1b, probably due to the additional vibrational freedom of 1c compared with 1b, as suggested by the zero-point vibrational energy calculations (see below). Chlorination of the 2,6-positions increased the fluorescence quantum yields of BODIPYs 2a-2c relative to **1a–1c** [17, 29, 31], with the exception of BODIPY **1b** which showed very high quantum yields in the absence of the 2,6-chlorines and slightly lower yields in the dichlorinated derivative. The electron-withdrawing effect of the chlorine atoms in general increases the fluorescence quantum yields due to the decrease in electronic charge density on the BODIPY, particularly at the meso-position [31]. In addition, dichlorinated BODIPY 2c showed very high fluorescence quantum yields in dichloromethane and toluene, but moderate yields in methanol, likely

**Table 1.** Experimental and calculated spectroscopic properties of BODIPYs in dichloromethane (DCM), toluene, and methanol (MeOH) at room temperature. All parameters are calculated at M06-2X/6-31+G(d,p) level. The leading transition is HOMO $\rightarrow$ LUMO for all calculated molecules

BODIPY	Solvent	Dipole moment (Debye)	$\lambda_{abs}$ (nm)		ε (M <sup>-1</sup> cm <sup>-1</sup> )	Oscillator strength	$\lambda_{em}$ (nm)		$\Phi_{ m f}^*$	Oscillator strength	Stokes shift (nm)	
			Exp	Calc	Exp	Calc	Exp	Calc	Exp	Calc	Exp	Calc
1a	CH <sub>2</sub> Cl <sub>2</sub>	6.33	502	435	95 200	0.638	512	478	0.64	0.774	10	43
	Toluene		504		104900		515		0.68		11	
	CH <sub>3</sub> OH	6.56	499	431	82900	0.614	509	488	0.52	0.818	10	57
1b	CH <sub>2</sub> Cl <sub>2</sub>	6.31	503	437	61700	0.599	512	480	0.94	0.744	9	43
	Toluene		505		98 500		514		0.97		9	
	CH <sub>3</sub> OH	6.57	500	434	82700	0.574	509	489	0.90	0.793	9	55
1c	$CH_2Cl_2$	5.91	512	444	35 900	0.510	522	488	0.71	0.624	10	44
	Toluene		515		36800		525		0.66		10	
	CH <sub>3</sub> OH	6.30	509	441	31800	0.485	518	499	ND	0.729	9	55
2a	CH <sub>2</sub> Cl <sub>2</sub>	6.50	527	450	55 600	0.668	542	492	0.78	0.787	15	42
	Toluene		531		29900		545		0.80		14	
	CH <sub>3</sub> OH	6.73	524	446	44 100	0.643	538	490	0.73	0.829	14	40
<b>2</b> b	$CH_2Cl_2$	6.51	529	452	44600	0.635	542	493	0.83	0.764	13	41
	Toluene		531		37900		544		0.96		13	
	CH <sub>3</sub> OH	6.75	525	448	45 700	0.610	538	502	0.81	0.814	13	54
2c	$CH_2Cl_2$	6.28	539	456	36 100	0.575	552	504	0.93	0.685	13	48
	Toluene		541		37600		554		0.98		13	
	CH <sub>3</sub> OH	6.62	535	452	36300	0.550	548	499	0.48	0.750	13	58

<sup>\*</sup>Fluorescein (0.90 in 0.1 M NaOH) and rhodamine 6G ( $\Phi_f$ = 0.94 in anhydrous ethanol) were used as the standard for BODIPYs **1a–1c** and **2a–2c**, respectively. ND = not determined due to poor solubility in the solvent.

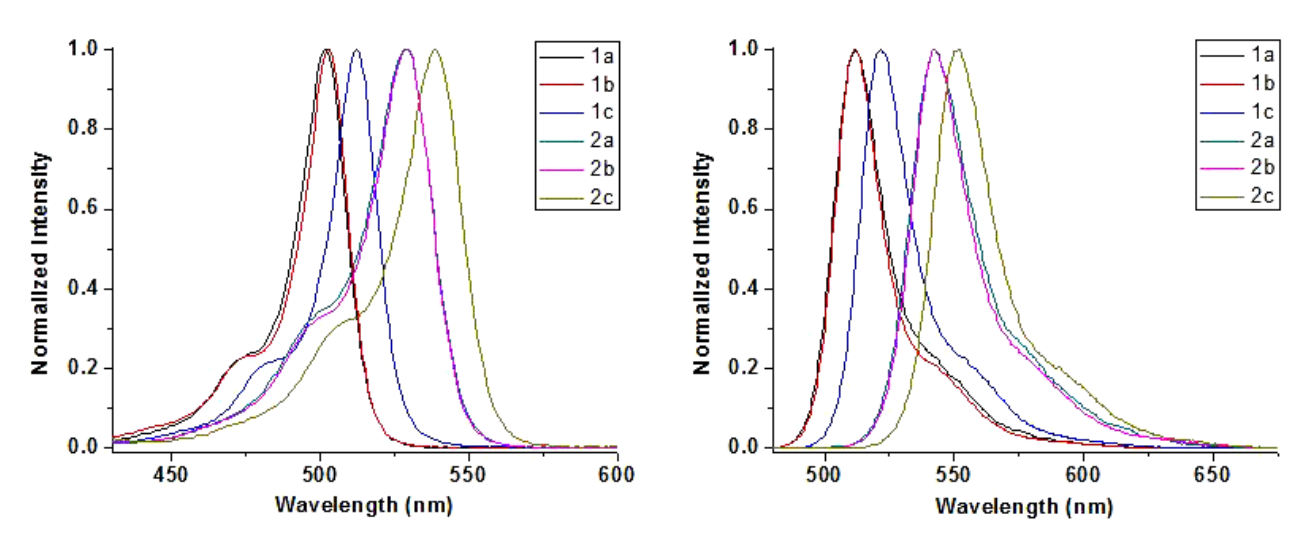


Fig. 3. Normalized UV-vis (left) and fluorescence (right) emission spectra of BODIPYs 1a-1c and 2a-2c in dichloromethane at room temperature

due to its lower solubility in this solvent (although slightly higher than 1c). These results are in agreement with previous reports showing that the nonradiative rate

constant decreases significantly with each chlorine atom introduced on the BODIPY [31].

# **Computational studies**

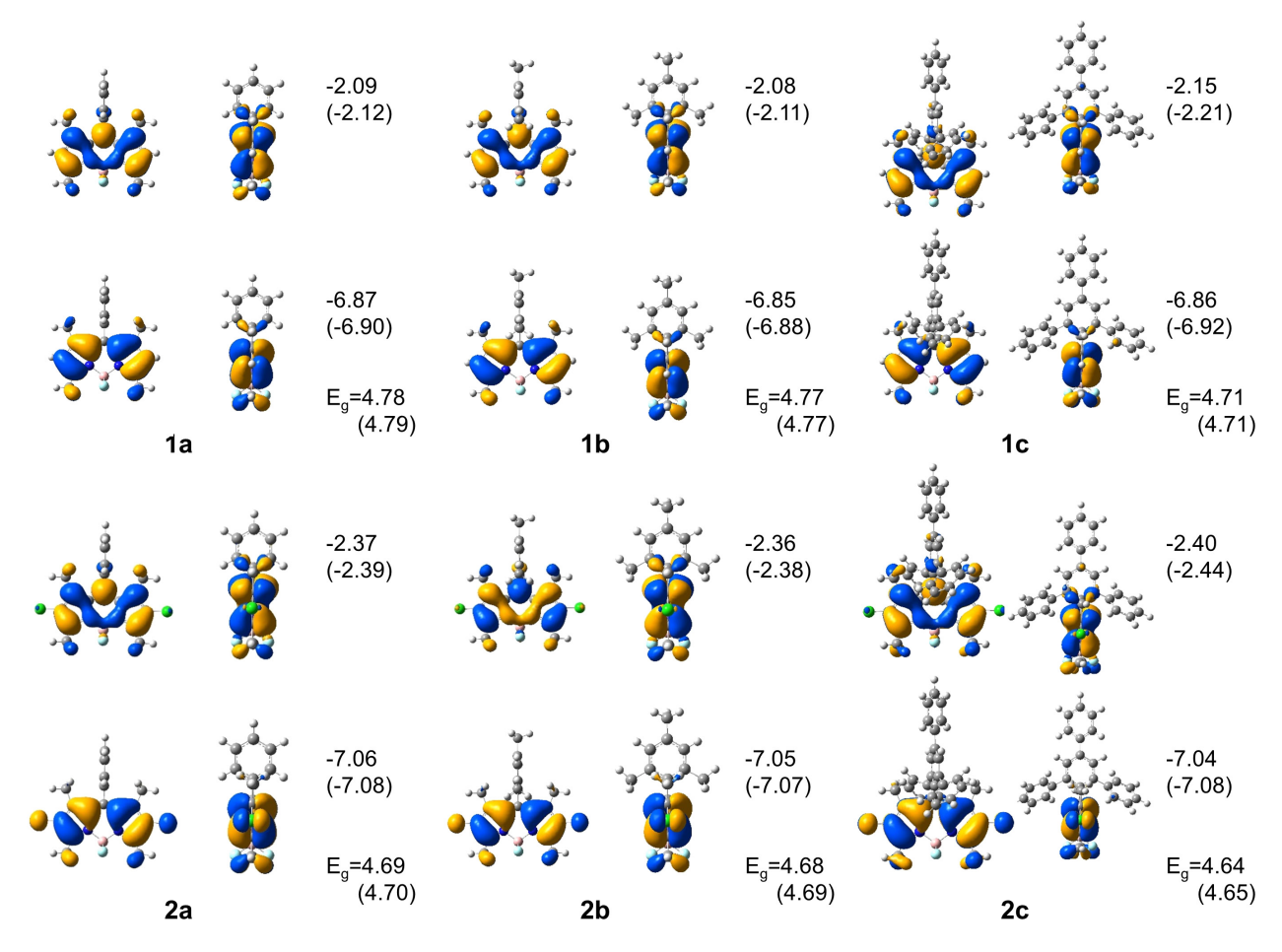


Fig. 4. Front view and side view of the frontier orbitals of BODIPYs 1a–1c and 2a–2c. Orbital and gap energies in eV. Modeled in dichloromethane (methanol)

To complement the experimental characterization, all BODIPYs were modeled computationally. The energies and shapes of the calculated frontier molecular orbitals in dichloromethane are presented in Fig. 4. The energy gap is also given. The shapes of HOMO and LUMO are similar in the entire series with little electron density located on the *meso*-substituent. The HOMOs of the 2,6-dichlorinated BODIPYs show electron density on the chlorine atoms that correspond to chlorine lone pairs. The orbital energies differ only slightly but are able to explain several experimental trends as described below.

Using dichloromethane as a solvent, the calculations confirm the experimentally observed red-shifted absorption peaks of BODIPYs **2a–2c** as compared to BODIPYs **1a–1c** (Table 1). As expected, the electron-withdrawing chlorine atoms at the 2,6-positions stabilize both the HOMO and LUMO, but the effect on the LUMO is more pronounced. As a result, the HOMO-LUMO gaps for **2a–2c** are about 0.1 eV smaller than those for **1a–1c**, which explains the observed red shifts of the absorption maxima wavelengths. The observed red shifts and HOMO-LUMO stabilizations are in agreement with previous studies [29, 31].

The effect of the *meso*-aryl substitution on orbital energies is very small. Still, the predicted red-shift from **1a** to **1b** to **1c** and **2a** to **2b** to **2c** confirms the experimental findings and is in agreement with the slightly decreased band gap, as seen in Fig. 4.

Using methanol instead of dichloromethane as the solvent stabilizes both HOMO and LUMO (Fig. 4). The effect on both orbitals is very similar but results in a slight increase in the HOMO–LUMO gap. This is in agreement with the observed small (3–4 nm) hypsochromic shifts of the maximum absorption wavelengths in methanol *vs.* dichloromethane (Table 1). In general, the solvatochromic shifts are complex in BODIPYs, and could involve contribution from polarity, polarizability, H-bond formation abilities, and electron-donor capacities of the solvent [32, 34].

The performed calculations suggest a slight lowering of the oscillator strengths from 1a to 1b to 1c and 2a to 2b to 2c, which is in agreement with the experimental molar absorptivities. The same trend is predicted for the fluorescence abilities of the synthesized BODIPYs. Indeed, experimentally, 1c is less fluorescent than 1b in dichloromethane and toluene. On the other hand,

the oscillator strengths are smaller in methanol than in dichloromethane, which might explain the lower fluorescence quantum yields observed for **1a** and **1b** and **2a–2c** in methanol. Polar solvents such as methanol are expected to decrease the fluorescence quantum yields due to increased solute–solvent interactions and higher probability for external conversion. Indeed, all BODIPYs from the series are polar with dipole moments ranging from 5.9 to 6.8 D (Table 1).

The lower fluorescence quantum yield observed for BODIPY 1c relative to 1b (Table 1) might be explained with the increased vibrational freedom of the larger size molecule. Indeed, zero-point vibrational energies increase from 0.3437 a.u. for 1a, to 0.4263 for 1b and 0.5859 a.u. for 1c. As discussed above, restricting the rotational and vibrational freedom of the *meso*-aryl substituent can play a substantial role in the observed fluorescence quantum yield due to decreased probability for non-radiative decay. The calculated rotational barrier for BODIPY 1a is 24.7 kcal/mol and involves distortion of the planarity of the BODIPY core (Fig. 5). 2,6-Dichloro substitution does not change the barrier significantly; it is calculated to be 23.5 kcal/mol for BODIPY 2a. Without the distortion (keeping the BODIPY core planar) the barrier for 1a is high at 46 kcal/mol, so likely distortion occurs upon rotation, since the distortion of the BODIPY core allows easier rotation of the phenyl group. Rotation of around 50° keeps the core planar but a distortion is observed after that which increases as the dihedral angle increases. Room temperature kinetic energy is enough to overcome barriers of roughly 20 kcal/mol. Therefore, the meso-phenyl group of BODIPY 1a most likely does not rotate completely at room temperature. However, a partial rotation to 80-85° is possible, in agreement with the dihedral angle observed by X-ray crystallography [16]. Since rotation of the meso-aryl group significantly influences the extent of the  $\pi$ -electron conjugation system [23], this rotational freedom is associated with

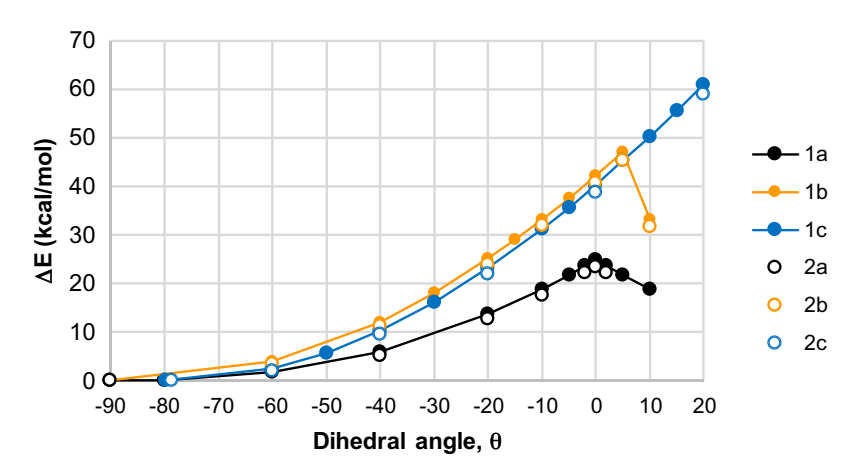


**Fig. 5.** Potential energy surface for the ground states of BODIPYs **1a–1c** and 2,6-dichloro-BODIPYs **2a–2c** as a function of the *meso*-aryl dihedral angle. Modeled in dichloromethane

lower quantum yields and likely explains the lower values observed for 1a in comparison with 1b and 1c. The presence of bulkier meso-8-aryl substituents, as in BODIPYs 1b and 1c makes the rotation more difficult, as demonstrated with the increased rotational barriers of 47.0 and more than 60 kcal/mol, respectively. Again, full rotation is not possible at room temperature, however, partial rotation at around 60-65° for 1b and at around 50-55° for 1c can be accomplished. The BODIPY core distortion starts around dihedral angle of 50° for 1b and 40° for 1c. Interestingly, the newly-synthesized BODIPY 1c exhibits an "umbrella-like" distortion as a result of the rotation. As the *meso*-8-(2.4.6-triphenylphenyl) group rotates, the 2,4,6-phenyls move up (away from the BODIPY core) to avoid the steric interaction. The calculated potential energy surface shows that increasing the dihedral angle from -80 to +60° still does not reach the energy maximum.

Previous studies [31] have suggested that the removal of electron density from the BODIPY core by electron-withdrawing substituents should be "beneficial for the fluorescence capabilities of the chlorinated derivatives because it should significantly reduce the deleterious influence of the phenyl free rotation on their photophysics." However, our studies of the potential energy surfaces of BODIPYs 1a–2c (see Fig. 5) demonstrate that the 2,6-dichloro substitution does not significantly affect the rotational barrier.

# **EXPERIMENTAL**

#### **Synthesis**

General. All commercially available reagents and solvents were purchased and directly used without purification. The reactions were monitored by analytical thin-layer chromatography using plastic-backed TLC plates 254 (precoated, 200 μm) from Sorbent Techno-

logies Co. Column chromatography was performed on silica gel 60 (230 × 400 mesh). NMR characterization of all products were conducted on an AVIII-400-3 Bruker spectrometer (400 MH for  $^{1}$ H, 128 MHz for  $^{11}$ B) and an AV500-PRODIGY Bruker spectrometer (126 MHz for  $^{13}$ C). Chemical shifts were recorded in  $\delta$  (ppm) relative to CDCl<sub>3</sub> 7.26 ppm ( $^{1}$ H), 77.0 ppm ( $^{13}$ C); CD<sub>2</sub>Cl<sub>2</sub> 5.30 ppm ( $^{1}$ H), 53.4 ppm ( $^{13}$ C) and BF<sub>3</sub>OEt<sub>2</sub> 0.00 ppm ( $^{11}$ B). BODIPYs **1a** [27, 35], **1b** [30, 36, 37], and **2a** [31, 38] were prepared as previously reported.

**BODIPY** 1c. To a mixture of 2,4,6-triphenylbenzaldehyde (100 mg, 0.3 mmol) and 2,4-dimethylpyrrole (68 mg, 0.72 mmol) dissolved in dichloromethane (15 mL), was added a

catalytic amount of TFA under argon and the final solution was stirred at room temperature for 8 h. 2,3-Dichloro-5,6dicyano-1,4-benzoquinone or DDO (68 mg, 0.3 mmol) was then added to the mixture in small portions. After 2 h of stirring, triethylamine (0.63 ml, 4.5 mmol) and BF<sub>3</sub>·OEt<sub>2</sub> (0.44 ml, 4.5 mmol) were added and the mixture left to react for 12 h before quenching with sat. NaHCO<sub>3</sub> solution. The organic phase was washed with water and brine, dried over anhydrous Na<sub>2</sub>SO<sub>4</sub>, and the solvent evaporated under vacuum. The crude product was purified by silica gel column chromatography using dichloromethane/hexane (1:1) as eluent. The title product was dried under vacuum for 2 h and obtained in 24% (40 mg) yield. <sup>1</sup>H-NMR (400 MHz,  $CD_2Cl_2$ )  $\delta$  7.89–7.68 (m, 4H), 7.49 (t, J = 7.5 Hz, 2H), 7.41 (t, J=7.3 Hz, 1H), 7.34-7.14 (m, 10H), 5.91 (s, 2H), 2.39 (s, 2H)6H), 1.68 (s, 6H). <sup>13</sup>C-NMR (126 MHz, CD<sub>2</sub>Cl<sub>2</sub>) δ 155.03, 142.13, 141.87, 141.11, 140.21, 139.64, 139.41, 132.84, 130.16, 129.08, 128.93, 128.51, 128.01, 127.53, 127.05, 121.07, 14.28, 13.87. <sup>11</sup>B-NMR (128 MHz, CD<sub>2</sub>Cl<sub>2</sub>) δ 0.31 (t, J = 32.8 Hz). MS (ESI-TOF) m/z [M + H]<sup>+</sup> 553.26327, calcd for  $C_{37}H_{31}BF_2N_2$ , 553.26275.

BODIPY 2b. To a stirred dichloromethane solution (5 ml) of BODIPY **2a** (20 mg, 0.054 mmol), was added trichlorocyanuric acid (9.5 mg, 0.041 mmol) and the color of the solution changed immediately. The reaction was quenched with sat. NaHCO<sub>3</sub> after TLC showed the full conversion of starting material to the desired product. The organic phase was washed with water and brine and dried over anhydrous Na<sub>2</sub>SO<sub>4</sub>. The organic solvent was removed under reduced pressure and the resulting residue was purified by silica gel column chromatography using dichloromethane/hexane (1:4) for elution. The title product was dried under vacuum and obtained in 76% (18 mg) yield.  $^{1}$ H-NMR (400 MHz, CDCl<sub>3</sub>)  $\delta$  6.98 (s, 2H), 2.58 (s, 6H), 2.36 (s, 3H), 2.08 (s, 6H), 1.38 (s, 6H). <sup>13</sup>C-NMR (126 MHz, CDCl<sub>3</sub>) δ 152.19, 142.67, 139.26, 137.21, 134.82, 130.33, 129.24, 128.86, 122.24, 21.24, 19.48, 12.43, 10.83. <sup>11</sup>B-NMR (128 MHz, CDCl<sub>3</sub>) δ 0.35 (t, J = 31.9 Hz). MS (ESI-TOF) m/z [M – H]<sup>+</sup> 415.13235, calcd for C<sub>22</sub>H<sub>23</sub>BCl<sub>2</sub>FN<sub>2</sub>, 415.13139.

*BODIPY* 2c. This compound was synthesized as described above using BODIPY 1c (20 mg, 0.036 mmol) and trichlorocyanuric acid (6.3 mg, 0.027 mmol) to afford the title product in 72% (16 mg) yield. <sup>1</sup>H-NMR (400 MHz, CD<sub>2</sub>Cl<sub>2</sub>) δ 7.79 (d, J = 8.8 Hz, 4H), 7.51 (t, J = 7.5 Hz, 2H), 7.43 (t, J = 7.3 Hz, 1H), 7.36–7.11 (m, 10H), 2.43 (s, 6H), 1.68 (s, 6H). <sup>13</sup>C-NMR (126 MHz, CD<sub>2</sub>Cl<sub>2</sub>) δ 151.96, 142.65, 141.21, 140.68, 139.81, 139.38, 136.74, 131.02, 129.30, 129.24, 129.00, 128.40, 128.22, 127.77, 127.11, 122.40, 12.16, 11.55. <sup>11</sup>B-NMR (128 MHz, CDCl<sub>3</sub>) δ -0.02 (t, J = 31.7 Hz). MS (ESI-TOF) m/z [M – F]<sup>+</sup> 601.18141, calcd for C<sub>37</sub>H<sub>29</sub>BCl<sub>2</sub>FN<sub>2</sub>, 601.17858.

# **Spectroscopic properties**

All absorption spectra were measured on a Varian Cary 50 spectrophotometer. Emission spectra were

recorded on a PerkinElmer LS55 spectrophotometer. The measurement was carried out using HPLC-grade  $CH_2Cl_2$  and toluene and quartz cuvettes (10 mm path length) at room temperature. The molar extinction coefficients was determined from the plots of absorbance (A = 0.05–0.8) vs. concentration. Dilute solution (0.01 < A < 0.05) was used to determine the relative fluorescence quantum yields ( $\Phi_{\rm f}$ ). Fluorescein ( $\Phi_{\rm f}$  = 0.90 in 0.1 M NaOH) and rhodamine 6G ( $\Phi_{\rm f}$  = 0.94 in anhydrous ethanol) were employed as the external reference.

#### X-ray crystallographic data

Diffraction data for 1c were collected at T=90 K on a Bruker Kappa Apex-II DUO diffractometer equipped with a CuK $\alpha$  microfocus source ( $\lambda=1.54184$  Å). Refinement was by full-matrix least squares, with H atoms in idealized positions, guided by difference maps. Crystal data:  $C_{37}H_{31}BF_2N_2$ , monoclinic space group  $P2_1/c$ , a=11.082 (3), b=14.305 (5), c=18.404 (6) Å,  $\beta=102.01$  (2)°, Z=4,  $\rho_{calcd}=1.286$  g cm<sup>-3</sup>,  $\mu(CuK\alpha)=0.66$  mm<sup>-1</sup>. A total of 30,118 data was collected at  $\theta_{max}=60.2^\circ$ . R=0.080 for 1973 data with  $F_o^2>2\sigma(F_o^2)$  of 4234 unique data and 383 refined parameters, CCDC 1957273.

#### Computational studies

The geometries of all BODIPYs were optimized at the B3LYP/6-31G(d,p) level [39–40] without symmetry constraints. The stationary points on the potential energy surface were confirmed with frequency calculations. The solvent effects were taken into account using the Polarized Continuum Model (PCM) [41]. The UV-vis absorption data were calculated using the TD-DFT method [42] at the M06-2X/6-31+G(d,p) level [43] as recommended in the literature [44]. All calculations were performed using the Gaussian 09 program package [45]. The *meso*-aryl rotational energies were obtained by scanning the aryl dihedral angle and optimizing the remaining degrees of freedom using B3LYP/6-31+G(d,p) level and redundant internal coordinates.

## **CONCLUSIONS**

A novel 1,3,5,7-tetramethyl-8-(2,4,6-triphenylphenyl)-BODIPY **1c** and its 2,6-dichloro analog **2c** were synthesized and their spectroscopic properties compared with those of *meso*-8-phenyl, *meso*-8-mesityl and their 2,6-dichloro BODIPY derivatives. The structures of all the BODIPYs were confirmed by <sup>1</sup>H, <sup>11</sup>B and <sup>13</sup>C-NMR spectroscopy, and by high-resolution mass spectrometry. In addition, for the new BODIPY **1c** the X-ray structure was obtained, showing this molecule to be more distorted from planarity than **1a** and **1b**, and bearing a smaller *meso*-aryl dihedral angle of *ca*. 75°. The spectroscopic properties of the BODIPYs were conducted in dichloromethane, toluene, and methanol solutions. The introduction of 2,6-dichloro

substituents on BODIPYs 1a–1c stabilizes the HOMO and LUMO, causing about 25 nm red-shifted absorptions and emissions of BODIPYs 2a–2c, while reducing the molar absorptivities. On the other hand, 2,6-dichloro substitution tends to increase the fluorescence quantum yields, particularly in the case of new BODIPY 2c, which displayed the highest quantum yields in dichloromethane and toluene of all BODIPYs investigated.

#### Acknowledgments

This work was supported by the National Science Foundation (CHE-1800126). The authors thank the Louisiana Optical Network Initiative (www.loni.org) for the use of their computer facilities.

#### **Supporting information**

<sup>1</sup>H-, <sup>13</sup>C-and <sup>11</sup>B-NMR spectra, UV-vis and fluorescence emission spectra for BODIPYs, and optimized Cartesian coordinates for the ground and excited states of **1c** and **2c** are given in the supplementary material. This material is available free of charge *via* the Internet at http://www.worldscinet.com/jpp/jpp.shtml. Crystallographic data for compound **1c** has been deposited at the Cambridge Crystallographic Data Centre (CCDC) under number CCDC 1957273. Copies can be obtained on request, free of charge, *via* http://www.ccdc.cam.ac.uk/data\_request/cif or from the Cambridge Crystallographic Data Centre, 12 Union Road, Cambridge CB2 1EZ, UK (Fax: +44 1223-336-033 or email: deposit@ccdc.cam.ac.uk).

# REFERENCES

- 1. Loudet A and Burgess K. *Chem. Rev.* 2007; **107**: 4891–4932.
- 2. Ziessel R, Ulrich G and Harriman A. *New J. Chem.* 2007; **31**: 496–501.
- 3. Ulrich G, Ziessel R and Harriman A. *Angew. Chem.*, *Int. Ed. Engl.* 2008; **47**: 1184–1201.
- 4. Boens N, Leen V and Dehaen W. *Chem. Soc. Rev.* 2012; **41**: 1130–1172.
- Kowada T, Maeda H and Kikuchi K. Chem. Soc. Rev. 2015; 44: 4953–4972.
- 6. Bañuelos J. Chem. Rec. 2016; 16: 335-348.
- 7. Lu H, Mack J, Nyokong T, Kobayashi N and Shen Z. *Coord. Chem. Rev.* 2016; **318**: 1–15.
- 8. Bertrand B, Passador K, Goze C, Denat F, Bodio E and Salmain M. *Coord. Chem. Rev.* 2018; **358**: 108–124.
- Bodio E, Denat F and Goze C. *J. Porphyrins Phthalocyanines* 2019; 23: Ahead of print, DOI: 10.1142/S1088424619501268.
- 10. Ali H, Ouellet R, van Lier JE and Guérin B. *J. Porphyrins Phthalocyanines* 2019; **23**: 781–796.
- 11. Li L, Nguyen B and Burgess K. *Bioorg. Med. Chem. Lett.* 2008; **18**: 3112–3116.

- 12. Jiao L, Yu C, Li J, Wang Z, Wu M and Hao E. *J. Org. Chem.* 2009; **74**: 7525–7528.
- 13. Zhang G, Wang M, Fronczek FR, Smith KM and Vicente MGH. *Inorg. Chem.* 2018; **57**: 14493–14496.
- 14. Wang M, Zhang G, Bobadova-Parvanova P, Merriweather AN, Odom L, Barbosa D, Fronczek FR, Smith KM and Vicente MGH. *Inorg. Chem.* 2019; **58**: 11614–11621.
- 15. Ziessel R, Goze C and Ulrich G. *Synthesis* 2007; **2007**: 936–949.
- 16. Wang H, Vicente MGH, Fronczek FR and Smith KM. *Chem. Eur. J.* 2014; **20**: 5064–5074.
- Zhao N, Xuan S, Fronczek FR, Smith KM and Vicente MGH. J. Org. Chem. 2015; 80: 8377–8383.
- 18. Deniz E, Isbasar GC, Bozdemir ÖA, Yildirim LT, Siemiarczuk A and Akkaya EU. *Org. Lett.* 2008; **10**: 3401–3403.
- 19. Uppal T, Bhupathiraju NDK and Vicente MGH. *Tetrahedron* 2013; **69**: 4687–4693.
- Zaitsev AB, Méallet-Renault R, Schmidt EY, Al'bina IM, Badré S, Dumas C, Vasil'tsov AM, Zorina NV and Pansu RB. *Tetrahedron* 2005; 61: 2683–2688.
- Zhao N, Vicente MGH, Fronczek FR and Smith KM. Chem — Eur. J. 2015; 21: 6181–6192.
- 22. Hu W, Lin Y, Zhang X-F, Feng M, Zhao S and Zhang J. *Dyes Pigm.* 2019; **164**: 139–147.
- 23. Kee HL, Kirmaier C, Yu L, Thamyongkit P, Youngblood WJ, Calder ME, Ramos L, Noll BC, Bocian DF and Scheidt WR. *J. Phys. Chem. B* 2005; **109**: 20433–20443.
- 24. Kuimova MK, Yahioglu G, Levitt JA and Suhling K. *J. Am. Chem. Soc.* 2008; **130**: 6672–6673.
- 25. Wang L, Xiao Y, Tian W and Deng L. *J. Am. Chem. Soc.* 2013; **135**: 2903–2906.
- Ogle MM, Smith McWilliams AD, Ware MJ, Curley SA, Corr SJ and Martí AA. J. Phys. Chem. B 2019; 123: 7282–7289.
- Gibbs JH, Robins LT, Zhou Z, Bobadova-Parvanova P, Cottam M, McCandless GT, Fronczek FR and Vicente MGH. *Bioorg. Med. Chem.* 2013; 21: 5770–5781.
- Mendonça GF, Sindra HC, de Almeida LS, Esteves PM and de Mattos MC. *Tetrahedron Lett.* 2009; 50: 473–475.
- LaMaster DJ, Kaufman NE, Bruner AS and Vicente MGH. J. Phys. Chem. A 2018; 122: 6372–6380.
- 30. Tsuchiya M, Sakamoto R, Shimada M, Yamanoi Y, Hattori Y, Sugimoto K, Nishibori E and Nishihara H. *Chem. Commun.* 2017; **53**: 7509–7512.
- 31. Duran-Sampedro G, Agarrabeitia AR, Garcia-Moreno I, Costela A, Bañuelos J, Arbeloa T, López Arbeloa I, Chiara JL and Ortiz MJ. *Eur. J. Org. Chem.* 2012; **2012**: 6335–6350.

- 32. López Arbeloa F, Bañuelos Prieto J, Martínez VM, Arbeloa López T and López Arbeloa I. *Chem-PhysChem* 2004; **5**: 1762–1771.
- 33. Qin W, Baruah M, Van der Auweraer M, De Schryver FC and Boens N. *J. Phys. Chem. A* 2005; **109**: 7371–7384.
- 34. Boens N, Wang L, Leen V, Yuan P, Verbelen B, Dehaen W, Van der Auweraer M, De Borggraeve WD, Van Meervelt L, Jacobs J, Beljonne D, Tonnelé C, Lazzaroni R, Ruedas-Rama MJ, Orte A, Crovetto L, Talavera EM and Alvarez-Pez JM. *J. Phys. Chem. A* 2014; **118**: 1576–1594.
- 35. Gabe Y, Urano Y, Kikuchi K, Kojima H and Nagano T. *J. Am. Chem. Soc.* 2004; **126**: 3357–3367.
- 36. Fu L, Jiang F-L, Fortin D, Harvey PD and Liu Y. *Chem. Commun.* 2011; **47**: 5503–5505.
- Martinez-Espinoza MI, Sori L, Pizzi A, Terraneo G, Moggio I, Arias E, Pozzi G, Orlandi S, Dichiarante V, Metrangolo P, Cavazzini M and Bombelli FB. Chem. Eur. J. 2019; 25: 9078–9087.

- 38. Wang X-F, Yu S-S, Wang C, Xue D and Xiao J. *Org. Biomol. Chem.* 2016; **14**: 7028–7037.
- 39. Lee C, Yang W and Parr R. *Phys. Rev. A* 1988; **38**: 3098.
- 40. Becke AD. J. Chem. Phys. 1993; 98: 1372-1377.
- 41. Tomasi J, Mennucci B and Cammi R. *Chem. Rev.* 2005; **105**: 2999–3094.
- 42. Bauernschmitt R and Ahlrichs R. *Chem. Phys. Lett.* 1996; **256**: 454–464.
- 43. Zhao Y and Truhlar DG. *Theor. Chem. Acc.* 2008; **120**: 215–241.
- 44. Le Guennic B and Jacquemin D. *Acc. Chem. Res.* 2015; **48**: 530–537.
- 45. Frisch M, Trucks G, Schlegel H, Scuseria G, Robb M, Cheeseman J, Scalmani G, Barone V, Mennucci B and Petersson G. *Gaussian Inc.*, Wallingford, CT 2009.